

Deposition dynamics of Na monomers and dimers on an Ar(001) substrate

P. M. Dinh^{a*}, F. Fehrer^b, P.-G. Reinhard^b, E. Suraud^a

^aLaboratoire de Physique Théorique, Université Paul Sabatier, CNRS, F-31062 Toulouse Cédex, France

^bInstitut für Theoretische Physik, Universität Erlangen, D-91058 Erlangen, Germany

Abstract

We study deposition dynamics of Na and Na₂ on an Ar substrate, both species neutral as well as charged. The system is modeled by a hierarchical approach describing the Na valence electrons by time-dependent density-functional theory while Na core, Ar atoms and their dynamical polarizability are treated by molecular dynamics. We explore effects of Na charge and initial kinetic energy of the impinging Na system. We find that neutral Na is captured into a loosely bound adsorbate state for sufficiently low impact energy. The charged monomers are more efficiently captured and the cation Na⁺ even penetrates the surface layer. For charged dimers, we come to different final configurations depending on the process, direct deposit of Na₂⁺ as a whole, or sequential deposit. In any case, charge dramatically amplifies the excitation of the matrix, in particular at the side of the Ar dipoles. The presence of a charge also enhances the binding to the surface and favours accumulation of larger compounds.

Key words: TDDFT, hierarchical approach, deposition dynamics, rare gas surface
PACS: 31.15.ee, 31.70.Hq, 34.35.+a, 36.40.Wa, 61.46.Bc

1. Introduction

Clusters on surfaces are a much studied subject due to its interesting perspectives for basic research and for applications to nano-structured materials [1,2]. One important aspect is here the synthesis of deposited clusters. Two different techniques have been developed, namely controlled growth of elementary units on a surface by molecular beam epitaxy (for a brief review, see e.g. [3]) or direct deposition of size-selected clusters on a substrate (see e.g. [4]). An interesting aspect also concerns a non-destructive deposition technique of metal clusters on metal surfaces that can be achieved by means of a thin rare gas film above the metal surface (see e.g. [5] and refs. therein). We take up this scenario

and aim here at a theoretical study of deposition of Na on a rare gas surface. Thereby we concentrate on the first stages of growth, the capture of atoms and molecules with particular emphasis on charged projectiles.

The theoretical description of deposition dynamics employs predominantly classical molecular dynamics with effective atom-atom forces, see [6]. This was done, e.g., for the deposition dynamics of Cu clusters on metal [7] or Ar [8] surfaces, and of Al or Au clusters on SiO₂ [9]. That, however, does ignore possible effects from electronic degrees of freedom, as it can become crucial in metal clusters, and the more so if a finite net charge is involved. One then better uses models which take care of the electronic degrees of freedom. Fully detailed calculations have been undertaken, e.g., for the structure of small Na clusters on NaCl [10] or the deposit dynamics of Pd clusters on a MgO substrate [11]. But the expense

* Corresponding author
Email-address : dinh@irsamc.ups-tlse.fr

for such fully fledged quantum simulations grows huge. These subtle models are hardly extendable to truly dynamical situations, to larger clusters or substrates, and to systematic explorations for broad variations of conditions. There thus exists a great manifold of approximations which aim at an affordable compromise between reliability and expense, often called quantum-mechanical-molecular-mechanical (QM/MM) models. They have been applied for instance to chromophores in bio-molecules [12,13], surface physics [14,15], materials physics [16,17,18,19], embedded molecules [20] and ion channels of cell membranes [21]. We take up here a QM/MM modeling which was developed particularly for the combination of Na clusters with Ar substrate [22,23,24]. This method has already been successfully applied to deposition dynamics on finite Ar clusters [25] or on Ar surfaces [26]. The originality of this approach lies in the fact that the substrate polarizability is treated dynamically, a key aspect as soon as charged species are considered. In this paper, as stated above, we focus on the basic initial stages, that is, deposition of a single Na atom or a Na dimer. We study the effect of the initial kinetic energy given to the deposited system and of its charge. We aim at the observation of different possible energy thresholds between regimes of dynamical bouncing, binding or inclusion of the Na in the Ar matrix. We also compare the direct deposition of Na₂ with the sequential process where the system is deposited atom by atom, in the spirit of the technique of atomic layer epitaxy or deposition [27].

2. Model

We start with a very brief summary of the hierarchical description of the combined NaAr system. We treat the metal atoms in full microscopic detail at the level of Time Dependent Local Density Approximation (TDLDA) for the valence electrons, coupled to Molecular Dynamics (MD) for the ions. Details on the successful TDLDA-MD approach for free clusters can be found in [28,29]. The substrate consists out of Ar atoms to which we associate classical degrees of freedom for position and dipole moment. The latter serves to take into account the dynamical polarizability of the substrate. The Ar atoms are coupled to the Na by long range polarization and some short range repulsion to account for the Pauli blocking of cluster electrons in the vicin-

ity of the Ar cores. The model is calibrated to measured properties of typical Na-Ar systems. We refer the reader to [22,23,30] for a detailed description of the model.

The Ar(001) surface is modeled through six layers of 8×8 Ar atoms. The atoms in the two lowest layers are frozen at bulk crystal positions. The layers are periodically repeated in both lateral directions, thus simulating bulk material in these two dimensions. The six-layer sample in vertical direction is finite but is sufficiently large. We have counterchecked that by repeating some calculations for eight layers (making 512 atoms). That did not make much a difference and the now dynamically free fifth and sixth layers did not acquire any sizeable amount of kinetic energy. Thus freezing them in the 384 atom sample is a good approximation, at least for qualitative purposes.

The dynamics is initialized by placing the projectile (Na atom, ion or dimer) at a distance of 20 a_0 from the surface and boosting it with a given initial kinetic energy E_0 , towards the substrate and along the direction (denoted by z in the following) normal to it. We analyze the subsequent dynamics in terms of detailed ionic and atomic coordinates as well as of the various parts of the kinetic energy.

3. Dynamical deposition of neutral Na on Ar surface

As a first test case, we study the deposition of a neutral Na atom. Figure 1 shows results for three different impact energies. The atom is captured by the surface for all initial kinetic energies $E_0 \leq 0.14$ eV. Above this value, after impact, the Na acquires a positive escaped velocity which does not change of sign with time later on. The projectile is thus reflected and the process turns into an inelastic collision. The threshold value of 0.14 eV looks low at first glance. It is, however, already larger than the energies of Ar binding (typically 0.05 eV) and of the NaAr dimer (0.005 eV). And even in the regime of capture, the atom can still have huge amplitudes in its first bouncing oscillations reaching far away from the surface which leaves these initial stages somewhat vulnerable against perturbations. Safe deposit with immediate binding would require very low impact energies. The Ar material is, in fact, rather repelling to one single neutral Na atom. The latter is just loosely tied to the surface and insertion inside is energetically much unfavourable. That changes for

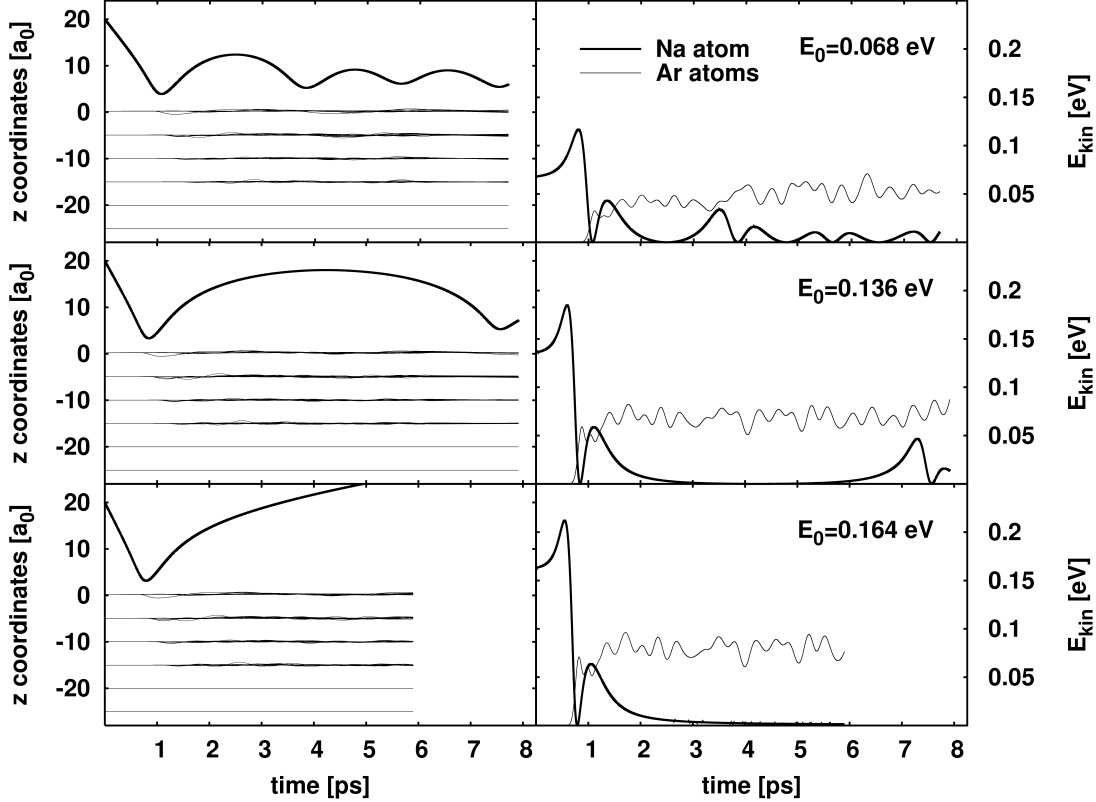


Fig. 1. Time evolution of z coordinates (left) and kinetic energies (right) for the collision or the deposition of a single neutral Na atom (thick line) on a planar Ar surface (Ar₃₈₄, faint curves), for three different impact energies E_0 , namely 0.218 eV (top), 0.136 eV (middle), and 0.068 eV (bottom).

Na clusters. Already small clusters as Na₆ or Na₈ are tightly captured in a wide range of impact energies [25,26] and they are also favourably embedded deep inside Ar material [31]. The difference stands in a larger polarizability of the cluster, due to the cooperative response of the valence electron cloud, while one single and tightly bound electron in the Na atom is too weak to develop a strong polarization. This difference shows the enormous importance of the polarization interaction in material combinations where metals and polarizable media are involved. We will see that again when considering charged projectiles farther below.

The reaction of the matrix seems weak when looking at the local positions in the left panels of figure 1. Nonetheless, one can spot a faint sound wave propagating through the layers and some oscillations. A more telling view of energy transport is provided by the right panels of figure 1 which show the evolution of kinetic energies for various impact energies. The patterns are to some extent all similar. About half of the initial kinetic energy of the Na atom is very

quickly transferred to Ar at first impact followed by a phase where kinetic energy is flowing away from the Na at a slower time scale. This second energy loss is due to the Na atom trying to escape against the attractive dipole force of the surface. A small fraction of the potential energy thus worked up is further transmitted to the kinetic energies of the Ar atom. After 2-3 ps, we have the typical result that almost all Na energy is transferred to the Ar substrate which seems to share it half and half into kinetic and potential energy. A quick note on the lowest right panel. It looks as if the Na atom had lost all its energy although the spatial picture (lowest left panel) shows final reflection. At second glance, we see that a small amount of kinetic energy remains steadily in the Na atom. It is obvious that just above threshold, we encounter a very inelastic collision.

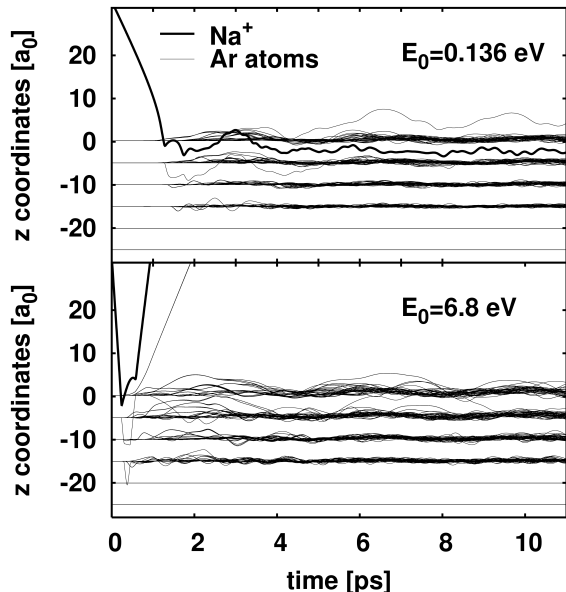


Fig. 2. Time evolution of z coordinates from the dynamical deposition of a Na^+ ion (thick lines) in Ar_{384} (thin curves) with two initial kinetic energy E_0 of 136 meV (top) and 6.8 eV (bottom).

4. Dynamical deposition of charged Na on Ar surface

4.1. The cation case

As clusters are usually manipulated as cations, it is especially interesting to consider the deposition problem with such charged species. We shall now consider this case in detail.

It should be noted that treating charged species requires a proper handling of the surface degrees of freedom. Accounting for the polarizability of Ar atoms dynamically, as we do in our model (see section 2), is here a crucial ingredient. It will thus also be interesting to look at how Ar dipoles respond to a deposition. A simple measure for this effect is the excitation energy of the dipoles which, in our model, scales with the square of the Ar dipole amplitudes. When depositing a neutral Na (cf. figure 1), the dipole excitation energy turns out to be vanishingly small, whatever the deposition energy. Thus we did not show it on the figure. Still, the effect of dipoles is known to be decisive, even at low energies, see for example in the analysis of optical properties of embedded metal clusters [24].

4.1.1. Time evolution of positions

We first view the deposition process in real space and plot again the z coordinates as a function of time for the deposition of Na^+ on $\text{Ar}(100)$. Figure 2 shows results for two typical deposition energies, one below and one above deposition threshold.

The lowest energy would correspond for the neutral Na atom to a situation just below threshold for capture (compare with middle panel in figure 1). The charge of the Na^+ enhances the attraction to the surface due to the Ar polarizability. This leads in the incoming stage to a much larger acceleration of the Na^+ ion towards the surface as compared with the neutral Na atom. But the now much larger kinetic energy at contact time (about 1 ps) does not cause immediate reflection. The large attraction enhances, in fact, capture. The ion uses its high kinetic energy at impact to overcome the short range repulsion of the Ar atoms and penetrates the first layer. It is then caught, after some oscillations forth and back, between first and second layers. In the first bounce back at around 3 ps, it makes space by kicking one Ar atom out of its position. With the creation of this vacancy, some rearrangements occur in the highest layers at a very slow time scale such that finally the Na^+ resides between first and second layers while one Ar atom is shifted out of the surface to what could be called the next upper Ar layer. There is however some uncertainty about the final fate of this atom. Indeed, although the way to equilibration is visible in the time evolution of the matrix kinetic energy (see top panel of figure 3, full thick line), the matrix is surely not thermalized yet. At 30 ps, the adatom still looks like an atom loosely adsorbed on the surface and will very probably remain so. But there is no guarantee that it does not finally escape by thermal agitation. Any weak external perturbation may destabilize that adsorbate.

The higher energy case, presented in the bottom panel of figure 2, displays reflection. In that case, the Na^+ is quickly ejected together with a few nearby Ar atoms. The remaining surface atoms accommodate the perturbation in a way similar to the lower energy case, however with somewhat larger oscillations.

4.1.2. Time evolution of energies

The evolution of atomic and ionic kinetic energies is plotted in the top panel of figure 3. It again shows first a large initial acceleration of the charged projectile caused by the attractive polarization interaction with the substrate. This effect is much larger than in the previous example with a neutral projec-

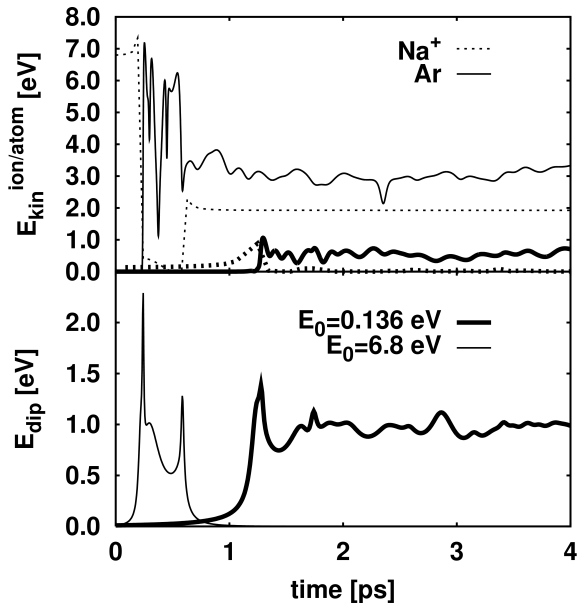


Fig. 3. Time evolution of typical energies involved in the dynamical deposition of a Na^+ ion in Ar_{384} , with two initial kinetic energies E_0 of 136 meV (thick curves) and 6.8 eV (thin curves). Top : Kinetic energies of Na^+ (dots) and Ar atoms (full lines) in the top panel. Bottom : Excitation energy of Ar dipoles for different E_0 as indicated.

tile. Much similar to the previous case is the immediate and large energy transfer to the substrate at the time of closest impact. The figure does now also show the kinetic energy of the Ar dipoles (see bottom panel).

Let us first discuss the low energy case. For the charged projectile, the energies of atoms and dipoles are of the same order of magnitude : For Ar atoms, about two thirds of the ion kinetic energy at impact (≈ 0.9 eV), while the Ar dipoles get an excitation energy up to about 1 eV. The energy gathered by the substrate comes from three sources : *i*) From direct conversion of the ion kinetic energy, *ii*) from release of potential energy due to deformation and rearrangements of the matrix, and *iii*) from the electrostatic influence of the inclusion of a positive charge into the matrix. Later, the remaining Na ion kinetic energy is quickly and almost completely taken up by the matrix in the tight bounces between the layers. It is remarkable to observe that the excitation of the matrix is as high for the atoms as for the dipoles. This demonstrates that the dynamic of dipole polarization plays a crucial role in the process and that a theoretical description has properly to take that into account. Omitting these degrees of freedom changes the deposition process completely, as has been also

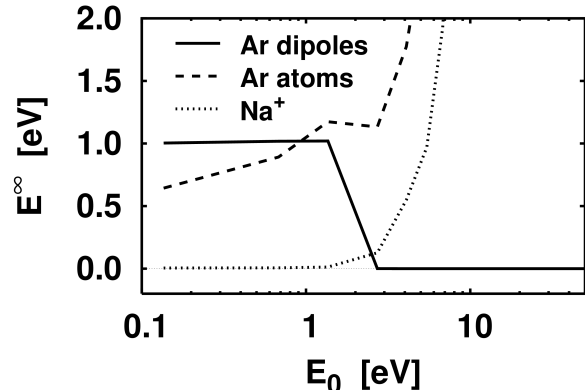


Fig. 4. Asymptotic kinetic energies of Na^+ (dotted) and of Ar atoms (dashes), and excitation energy of Ar dipoles (full line) as a function of initial kinetic energy E_0 of the Na^+ projectile.

shown in the case of Na clusters [26].

The higher energy case displays another interesting feature. At first glance, the dipole energy vanishes asymptotically, different from the low energy case. In fact, a closer look at the curve shows that this energy reaches temporarily very high values, before the few Ar atoms are emitted. It is thus likely that the few emitted atoms were precisely the ones which had the largest dipoles. A more detailed inspection of the spatial distribution of dipole energies confirms that.

4.1.3. Systematics in deposition energy

It is finally instructive to analyze the trends of deposition dynamics by considering the energetics as function of the initial kinetic energy of the projectile E_0 . Figure 4 shows the asymptotic kinetic energies of Na^+ , Ar atoms and excitation energy of Ar dipoles as a function of E_0 . The pattern indicate a dramatic change around $E_0 \approx 2.7$ eV, which is the transition point from capture to reflection of the impinging Na^+ . Above that critical energy, the outgoing kinetic energy of the Na^+ increases linearly with E_0 . The same holds for the energy of the Ar atoms because it is then dominated by the few atoms which are accompanying the departing ion. Below the threshold, these quantities also show a monotonous increase with impact energy. Most remarkable is the behaviour of the Ar dipoles which differs essentially from the two other quantities. Below threshold, when Na^+ ion is captured by the substrate, the Ar dipoles acquire an energy which seems to depend only on the net charge and not on the initial kinetic energy. Above threshold, the Ar

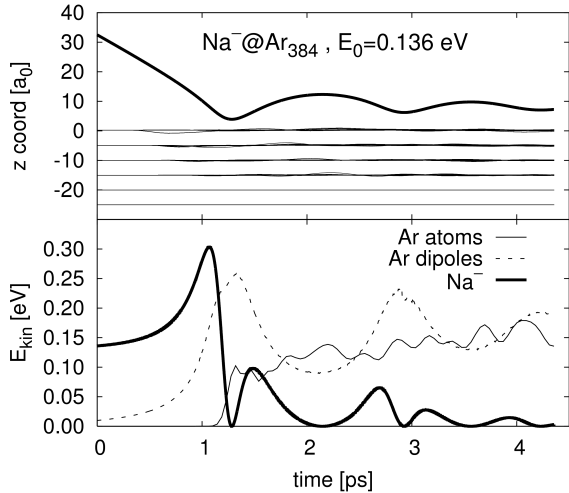


Fig. 5. Dynamical deposition of Na^- (thick lines) in Ar_{384} (thin curves) with an initial kinetic energy of 136 meV. z coordinates (top) and kinetic energy (bottom) of single Na and Ar matrix as a function of time.

dipole energy vanishes because the Na^+ finally escapes from the surface. Comparing with the bottom panel of figure 3, sharp peaks in the Ar dipole energy appear precisely when the Na^+ is in the vicinity of the surface and later on, the excitation energy rapidly decreases towards zero as the Na^+ moves away.

A final word has to be added about the reflection threshold we found around 2.7 eV. In the bottom panel of figure 2, we clearly notice the bouncing of the propagating wave in the Ar substrate at the level of the fifth layer. We recall that this layer, as well as the sixth layer, are fixed, for reasons of computational expense. The value for the reflection threshold, found here at $E_0 \approx 2.7$ eV, has thus to be taken with care. We checked the case of deposition of Na^+ with precisely this initial kinetic energy on Ar_{512} (six active layers plus two fixed ones) rather than Ar_{384} . Here the projectile is still captured and reflection emerges at higher initial energies. However, the qualitative features of deposition dynamics and trends remain the same although the threshold value is somewhat shifted.

4.2. The anion case

The other choice for a charged monomer is a Na^- anion. Figure 5 shows the result, this time again at the threshold energy for the neutral case, $E_0 = 0.136$ eV. The attraction for polarization potentials is as

large as it was for the Na^+ cation. But the doubly charged electron cloud experiences a full load of the Pauli repulsion from the Ar cores which is built into the short-range part of the effective electron-Ar interaction. As a consequence, the Na^- is blocked by the surface and will not penetrate into the material. On the other hand, the long-range attraction persists. Thus the anion is very efficiently captured at a safe distance from the surface. In comparison with the neutral case, there are no noteworthy amplitudes in the bouncing oscillations. Thus the anion comes quickly to a rest. In comparison to the cation case, the impact phase is much earlier stopped such that the anion could not acquire so much kinetic energy. This, in turn, leaves less energy to be absorbed by the substrate. The pattern of energy transport in the Ar atoms are similar to the neutral case: Half of the energy is immediately transferred at first impact and the other bits with each bounce. However, because of the negative charge, the Ar dipoles experience a much larger excitation and acquire a kinetic energy five or six orders of magnitude higher than in the case of the neutral Na deposition. Note finally that the time scale is also different because the bounces recur much more frequently.

For both charged cases, we mention that the threshold for capture is much higher than for the neutral cluster (not shown). And there is actually no regime of inelastic reflections. Enhancing the impact energy further to force reflection leads into a regime where a whole surface area is destroyed. This is similar to our findings for deposition of Na clusters [26].

5. A simple analysis of the results

It is, finally, instructive to interpret the above observed findings in terms of energy surfaces. To that end, we have computed the energy of Na, Na^+ or Na^- for systematically varied distances to the surface, keeping the distance and the atomic positions frozen while allowing the polarizabilities to adjust to the given configurations. This will provide an estimate of how far or close we are to (a)diabaticity in the deposition scenarios explored above. The energy surfaces for Na, Na^+ and Na^- on $\text{Ar}(001)$ are plotted in figure 6. The “static” results are qualitatively compatible with our fully dynamical calculations. Let us, for example, take the case of neutral Na. A faint minimum is found at a distance of about $7.5 a_0$ with a binding energy of -52 meV. This has

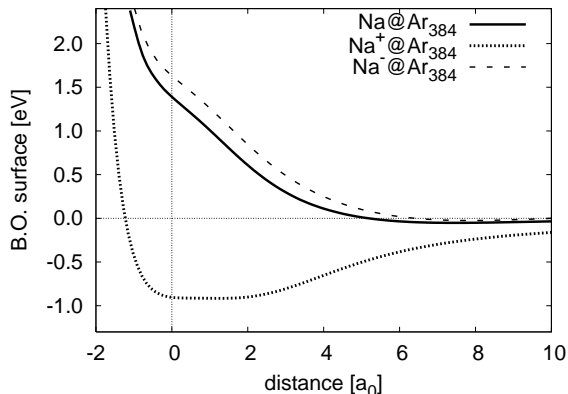


Fig. 6. Potential energy surface of neutral Na, Na^+ and Na^- on Ar_{384} , calculated with fixed Ar atoms.

to be compared with the threshold for reflection at 136 meV that we found in our dynamical calculations. This is 2–3 times larger than the “static” value but the orders of magnitude are similar. The same qualitative conclusion holds true for Na^+ and Na^- .

At a quantitative level, one has to note that there remains sizable differences between the static and dynamical results. This is an expected and welcome feature showing that, at least in the deposition energy range we consider, there remain genuine dynamical effects which cannot be simply evaluated without a proper account of dynamics. The point was rather obvious from the behavior of Ar atoms and dipoles as is particularly clear from figures 2 and 3.

The site dependence on the deposition has also been explored in this “static” way. The dynamical results presented in the previous sections all start from a projectile initially positioned above a hollow site in the first layer, but above on Ar atom in the second layer. We checked that changing the deposition site of course modifies the threshold in initial kinetic energy E_0 for the observation of the reflection. This, however, does not change qualitatively our findings. This is also compatible with the results on deposition of Na_6 on Ar clusters [25] and Ar surface [26], which show only weak dependence on implantation site.

6. Dynamical deposition of Na dimer

Not surprisingly, the effect of the charge is thus determinant for the fate of the deposited atom. In the same spirit, we have compared the cases for the dimers, Na_2 and Na_2^+ . The results are shown in the

top panels of figure 7. As for a single atom, the charged dimer sticks more closely to the Ar surface than the neutral Na_2 . Note that in both cases the dimers are not strongly perturbed. More precisely, the dimer bond lengths exhibit some oscillations but remain almost unchanged as compared to the free value : the Na_2^+ is slightly longer (+2 %), while the Na_2 bond length decreases by 4.5 %. The matrix shows more perturbation than in the previous cases with a single Na projectile. Two atoms have simply more impact which is fully downloaded into the matrix. Comparing the two dimers, we see that Na_2^+ attaches more tightly to the Ar surface which is, again, due to the larger attraction. However, the positively charged Na_2^+ stays above the surface and does not manage to dive below as the Na^+ did.

There is an alternative option to bring a dimer onto the surface, that is, sequential deposit of monomers. Particularly interesting is here the case where a Na^+ cation was deposited first and where, in a second round, a neutral Na atom is attached. The left lower panel of figure 7 shows that process. To produce the corresponding initial state, we take the final state of Na^+ deposition (see top panel of figure 2), remove the Ar adatom, relax the remaining configuration by cooling, and inject a neutral Na atom a distance of 15 a_0 from the surface with our meanwhile standard impact energy of 0.14 eV. The new Na atom is captured with small remaining oscillations. Compared with the direct deposition of Na_2^+ (top left panel of same figure), the charged dimer is more deeply bound with one leg residing below the surface. We also observe that its bond length is almost unchanged (-0.23%) with respect to the value of the free charged dimer. The example thus demonstrates that the final state can depend sensitively on the production process.

One could now hope that neutralization of that immersed Na_2^+ leads to an equally deep bound Na_2 dimer. To that end, we take the final state from the previous sequential deposit (at the end time in the lower left panel), cool the obtained configuration, and add an electron in the electronic ground state of the tied dimer with yet fixed ionic configuration. Then we release the system to fully free electronic, ionic, and atomic dynamics. The result is shown in the right lower panel of figure 7. The now neutral dimer pops up out of the surface and performs bouncing oscillations with large amplitude about the final stage of $\text{Na}_2\text{Ar}_{383}$ which was also obtained by direct deposit of Na_2 , see upper right panel. The minor difference with the now missing adatom plays

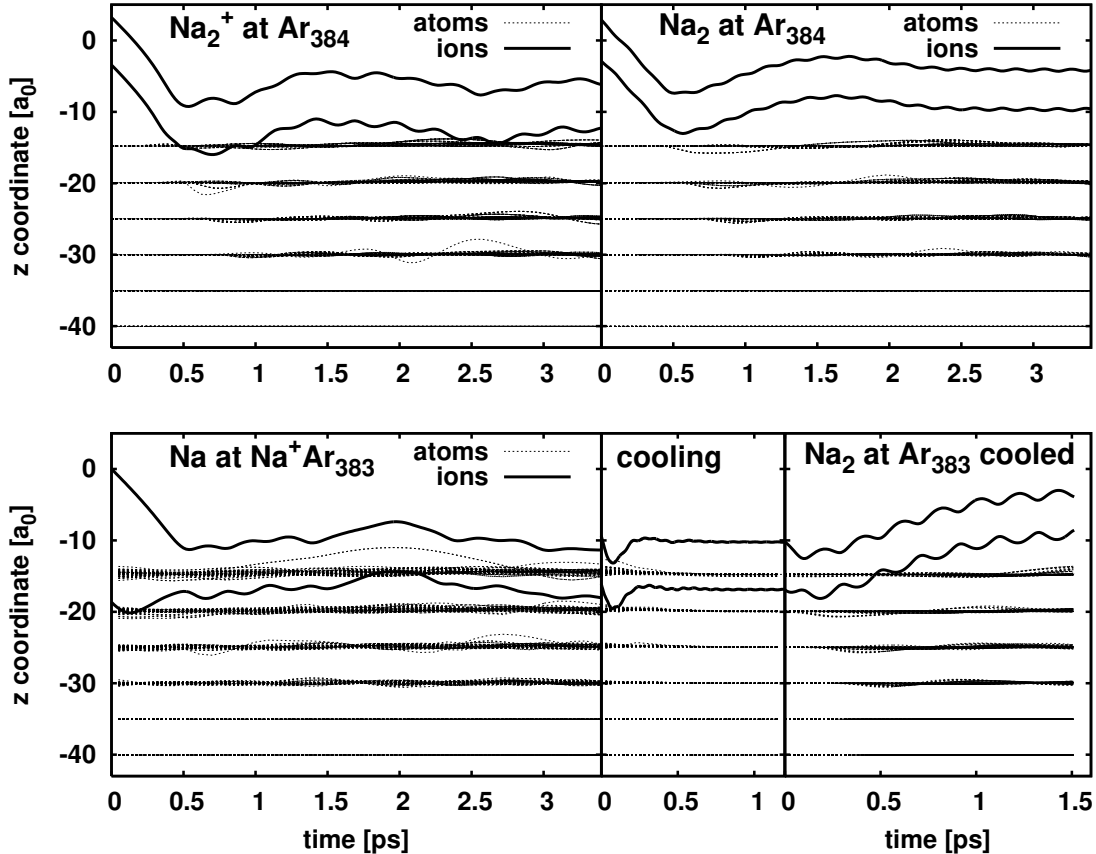


Fig. 7. Dynamical deposition of charged or neutral Na_2 with an initial kinetic energy of 136 meV/ion. Time evolution of ionic (thick lines) and atomic (dotted lines) z coordinates are shown. Top : direct deposition of Na_2^+ (left) and Na_2 (right) on Ar_{384} . Bottom, sequential deposition of Na^+ and then of neutral Na on Ar_{383} (left) and subsequent dynamics of the obtained Na_2^+ which is preliminary neutralized (right).

little role for the comparison. There are fast oscillations of the dimer bond length. These emerge because the neutral dimer has a smaller bond length than the charged one from which it was started. Note that these bond-length oscillations persist for long. This indicates that energy transfer from intrinsic ionic motion to the substrate is very slow, a feature which was also observed for larger clusters in Ar substrate [30].

In order to quantify the dynamics of dimer deposition in simple terms, we have plotted in figure 8 their center-of-mass (c.o.m.) z coordinate as a function of time. This complements the previous, more detailed, figures and allows a more direct comparison between the various cases. The lower panel shows direct deposit of neutral dimer as well as charged dimer and sequential deposit leading to a charged dimer. The trend is obvious : Binding stays 28 % closer to the surface for the charged dimer compared

with the neutral one, and sequential deposit brings it even closer (of about 60 %) so that the dimers center lies almost at the surface. For completeness, we also show in the upper panel the evolution of the re-neutralized charged dimer. The return to the equilibrium position of the directly deposited neutral dimer is visible as well as the still large oscillations about that point. Significant energy transfer happens only at the bouncing points and the long time span per bounce lets us predict a very slow relaxation needing about hundreds of ps.

7. Conclusion

To conclude this paper, we have studied deposition of Na atoms, Na ions and Na dimers on $\text{Ar}(001)$ substrate, using a hierarchical approach with time-dependent density-functional theory for the Na electrons coupled to molecular dynamics for the Na ions

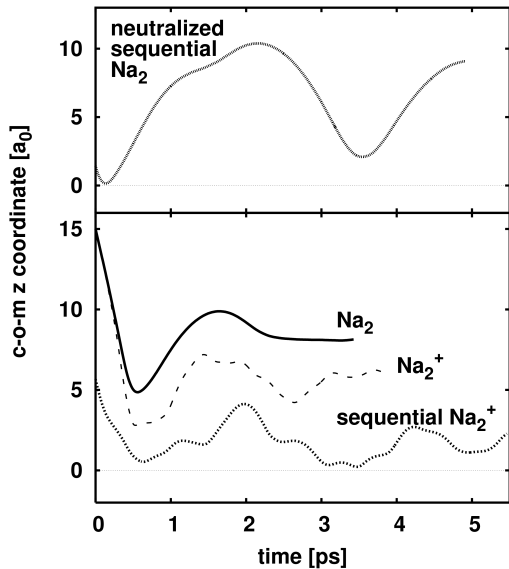


Fig. 8. Time evolution of the center of mass z -coordinate, relative to the Ar surface (here at $z = 0$), in a dynamical deposition of various Na dimers, as indicated.

and Ar atoms as well as dipole moments. We have paid particular attention to the effect of charged projectiles. We have found that the neutral Na is not likely to penetrate into the Ar matrix and sticks loosely to the Ar surface for initial kinetic energy lower than 0.14 eV while it is inelastically reflected for larger energies. A Na^+ cation behaves much differently. It is tightly captured and even penetrates the surface to reside finally between surface and next layer. The Ar surface undergoes strong perturbations and displaces one Ar atom to an adatom site. At a given size of Ar substrate, we found a reflection threshold twenty times larger for Na^+ than for neutral Na. Different is the behavior for the negatively charged Na^- anion. It is also tightly bound. But the strong electron-Ar repulsion keeps it safely above the surface. The deposition of Na dimers shows similar trends as for the atom. The charged dimer is closer bound than the neutral one. It stays, however, fully outside the substrate. The alternative process of sequential deposit produces a different final state for the charged Na_2^+ dimer. The lower ion of the dimer is placed now below the surface while the upper one stays just above. The final state obviously depends on the pathway of the process. It was, however, not possible to keep a neutral dimer in that close contact with the surface. Re-neutralizing the close Na_2^+ configuration leads back to the Na_2 outside the surface at a distance which was obtained also by direct deposit of Na_2 . After all, the results

show that charge makes a huge difference in connection with polarizable media as, e.g., Ar substrate. It acts to some extent as a catalyst for capture. The studies will be continued with larger samples to explore different scenarios for producing deposited clusters.

Acknowledgments: This work was supported by the DFG, project nr. RE 322/10-1, the French-German exchange program PROCOPE nr. 07523TE, the CNRS Programme “Matériaux” (CPR-ISMIR), Institut Universitaire de France, the Humboldt foundation, a Gay-Lussac price, and the French computational facilities CalMip (Calcul en Midi-Pyrénées), IDRIS and CINES.

References

- [1] H. Haberland (Ed.), *Clusters of Atoms and Molecules 2- Solvation and Chemistry of Free Clusters, and Embedded, Supported and Compressed Clusters*, Vol. 56, Springer Series in Chemical Physics, Berlin, 1994.
- [2] C. Binns, *Surf. Sci. Rep.* 44 (2001) 1.
- [3] H. Brune, *Metal Clusters at Surfaces, Structures*, Springer, Berlin, 2000.
- [4] W. Harbich, *Metal Clusters at Surfaces, Structures*, Springer, Berlin, 2000.
- [5] J. T. Lau, A. Achleitner, H. U. Ehrke, U. Langenbuch, M. Reif, W. Wurth, *Rev. Sci. Instrum.* 76 (2005) 063902.
- [6] C. Xirouchaki, R. E. Palmer, *Vacuum* 66 (2002) 167.
- [7] H.-P. Cheng, U. Landman, *J. Phys. Chem.* 98 (1994) 3527.
- [8] M. Ratner, W. Harbich, S. Fedrigo, *Phys. Rev. B* 60 (1999) 11730.
- [9] S. Takami, K. Suzuki, M. Kubo, A. Miyamoto, *J. of Nanoparticle Res.* 3 (2001) 213.
- [10] H. Häkkinen, M. Manninen, *J. Chem. Phys.* 105 (1996) 10565.
- [11] M. Moseler, H. Häkkinen, U. Landman, *Phys. Rev. Lett.* 89 (2002) 176103.
- [12] N. Gresh, D. R. Garmer, *J. Comp. Chem.* 17 (1996) 1481.
- [13] E. Tapavicza, I. Tavernelli, U. Rothlisberger, *Phys. Rev. Lett.* 98 (2007) 023001.
- [14] A. Nasluzov, K. Neyman, U. Birkenheuer, N. Rösch, *J. Chem. Phys.* 115 (2001) 17.
- [15] C. Inntama, L. V. Moskaleva, I. V. Yudanov, K. M. Neyman, N. Röscha, *Chem. Phys. Lett.* 417 (2006) 515.
- [16] A. Rubio, L. Serra, *Phys. Rev. B* 48 (1993) 18222.
- [17] L. I. Kurkina, O. V. Farberovich, *Phys. Rev. B* 54 (20) (1996) 14791–14795.
- [18] J. Lermé, B. Palpant, B. Prével, M. Pellarin, M. Treilleux, J. L. Vialle, A. Perez, M. Broyer, *Phys. Rev. Lett.* 80 (1998) 5105.
- [19] J. Lermé, *Euro. Phys. J. D* 10 (2000) 201.

- [20] M. Sulpizi, U. Röhrig, J. Hutter, U. Rothlisberger, *Int. J. Quantum Chem.* 101 (2005) 671.
- [21] D. Bucher, S. Rauegi, L. Guidoni, M. D. Peraro, U. Rothlisberger, P. Carloni, M. L. Klein, *Biophys. Chem.* 124 (2006) 292.
- [22] F. Dupl e, F. Spiegelmann, *J. Chem. Phys.* 105 (1996) 1492.
- [23] B. Gervais, E. Giglio, E. Jaquet, A. Ipatov, P.-G. Reinhard, E. Suraud, *J. Chem. Phys.* 121 (2004) 8466.
- [24] F. Fehrer, P.-G. Reinhard, E. Suraud, E. Giglio, B. Gervais, A. Ipatov, *Appl. Phys. A* 82 (2005) 151.
- [25] P. M. Dinh, F. Fehrer, G. Bousquet, P.-G. Reinhard, E. Suraud, *Phys. Rev. A* 76 (2007) 043201.
- [26] P. M. Dinh, F. Fehrer, P.-G. Reinhard, E. Suraud, *Eur. Phys. J. D* 45 (2007) 415.
- [27] T. Suntola, *Atomic Layer Epitaxy*, Blackie, Glasgow, 1990.
- [28] F. Calvayrac, P.-G. Reinhard, E. Suraud, C. A. Ullrich, *Phys. Rep.* 337 (2000) 493.
- [29] P.-G. Reinhard, E. Suraud, *Introduction to Cluster Dynamics*, Wiley, New York, 2003.
- [30] F. Fehrer, P.-G. Reinhard, E. Suraud, *Appl. Phys. A* 82 (2006) 145.
- [31] F. Fehrer, P. M. Dinh, P.-G. Reinhard, E. Suraud, *Phys. Rev. B* 75 (2007) 235418.